



Two cyanide-bridged compounds composed of Schiff base–manganese(III) building block with dicyanamido and hexacyanocobaltate(III) as ligands: Crystal structure, thermostability and magnetic property



Xiang-Yu Liu^{a,b,1}, Lin-Qiang Duan^{a,1}, Qing Wei^{a,*}, San-Ping Chen^{a,*}

^a Key Laboratory of Synthetic and Natural Functional Molecule Chemistry of Ministry of Education, College of Chemistry and Materials Science, Northwest University, Xi'an 710069, China

^b School of Chemistry and Chemical Engineering, Ningxia University, Yinchuan 750021, China

ARTICLE INFO

Article history:

Received 1 July 2014

Received in revised form 2 September 2014

Accepted 4 September 2014

Available online 16 September 2014

Keywords:

Cyanide ligands

Manganese

Schiff-base ligands

Thermostability

Magnetic property

ABSTRACT

Two new cyanide-bridged compounds, $[\text{Mn}(\text{L})(\mu_{1,3}\text{-N}(\text{CN})_2)]_n$ (**1**) and $\{[\text{Mn}_2(\text{L})_2(\text{H}_2\text{O})_2]\text{K}(\text{H}_2\text{O})_2\text{Co}(\text{CN})_6\}_n$ (**2**). ($\text{H}_2\text{L} = \text{N,N}'\text{-bis-5-chloro-salicylidene-1,2-diaminoethane}$), are synthesized and structurally characterized. Single-crystal X-ray diffraction analysis reveals that compounds **1** and **2** are composed of interesting 1D chain-like structure in which the manganese center is hexa-coordinated in the distorted octahedral geometry. In compound **1**, Mn(III) ions are bridged by $\text{N}(\text{CN})_2^-$ ligands with $\mu_{1,3}$ modes, while two CN^- groups in $\text{Co}(\text{CN})_6^{3-}$ ligand bridge two Mn(III) ions leading to a heterometallic trinuclear unit in compound **2**, several of the units are further connected by the linkage of CN^- groups and K(I) ions to form the chain-like structure. TGA results indicate that two compounds possess excellent thermostabilities. Magnetic measurement demonstrates that compounds **1** and **2** perform antiferromagnetic interaction with the coupling parameters (J) of -0.722 and -0.849 cm^{-1} , respectively. Magneto-structural correlation has been discussed as well.

© 2014 Elsevier B.V. All rights reserved.

1. Introduction

Rational design and construction of magnetic transition-metal coordination polymers, especially low-dimensional magnetic materials such as single-molecule magnets (SMMs) and single-chain magnets (SCMs), have attracted great attention because of their potential in the fields of high-density storage devices, molecular electronics and so on [1–15]. Up to now, remarkable progress has been achieved on this field, serving as the typical example of lots of relevant one-dimensional (1D) transition-metal compounds with fascinating molecular structures and magnetisms [16–19]. The magnetic properties of chain-like compounds largely depend on intrachain interaction which is effectively effected by short bridged ligands such as cyano, azido, hydroxyl, carboxyl and thiocyanate because of these ligands provide unique feature for transmitting magnetic coupling between adjacent spin centers [20,21]. In particular, the cyano group has been used extensively as a practicable and versatile mediator for magnetic coupling in

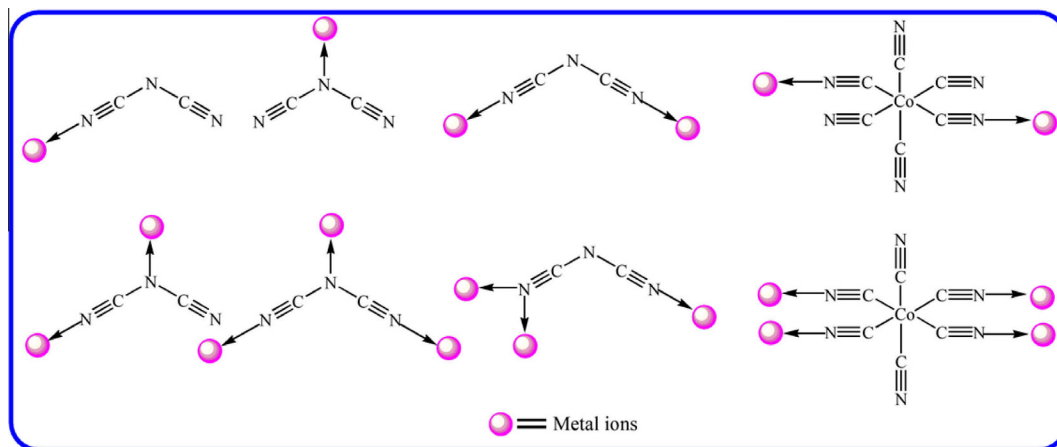
supramolecular chemistry and crystal engineering [22]. The cyanide-bridged compounds known show a wide range of magnet types, including metamagnets [23,24], room-temperature magnets [25,26], SMMs [27,28], and SCMs [29,10,30]. In light of our continuing interest in this field, we are committed to developing the system to the dicyanamido $[\text{N}(\text{CN})_2]^-$ and paramagnetic $[\text{Co}(\text{CN})_6]^{3-}$ building block which can act as important part in uni-, bi-, tridentate manner and both of its homo- and heteroleptic compounds, producing various topologies and intriguing magnetic properties (Scheme 1) [31,32].

According to the cyano-bridged compounds reported previously, magnetic assemblies based on hexa-coordinated Mn(III) ions are great significant because of the Mn(III) ions can not only act as the high spin carrier ($S = 2$) but also provide the source of uniaxial magnetic anisotropy [33,34]. Accordingly, besides introducing the cyano-bridged ligands to transmit the magnetic coupling between Mn(III) ions [35], it is also considerable to employ suitable coligand for obtaining expected magnetic Mn(III) compounds with favorable geometry [36]. As is well known, tetradentate salen type Schiff base (SB) derivative is the popular chelating ligand which has an inner site in the N_2O_2 chelating centers to bind metal cations and often serves as coligand in building coordinating polymers

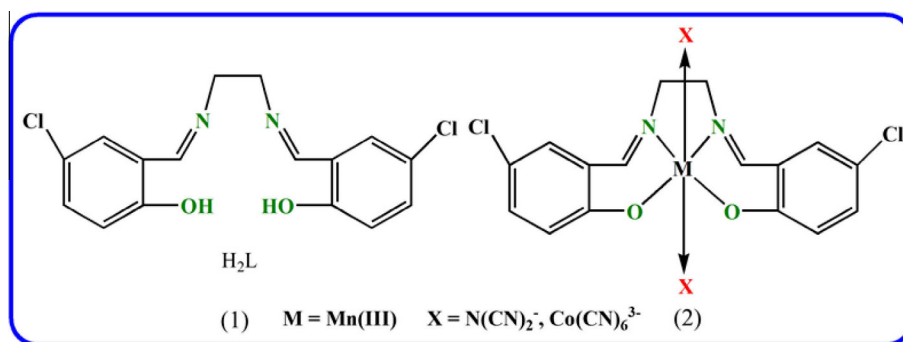
* Corresponding authors. Tel./fax: +86 029 88302604.

E-mail addresses: weiqq@126.com (Q. Wei), sanpingchen@126.com (S.-P. Chen).

¹ These authors have equal contribution to this work.



Scheme 1. Various dicyanamide and hexacyanocobaltate bridging modes.



Scheme 2. Representation of the ligand H_2L and simple chemical structure of the compounds.

(Scheme 2) [37]. All in all, it is meaningful for ongoing research to promote the development of the cyano-bridged magnetic materials based on the consideration above.

Fortunately, we successfully obtained two new cyano-bridged 1D compounds, $[Mn(L)(\mu_{1,3}-N(CN)_2)]_n$ (**1**) and $\{[Mn_2(L)_2(H_2O)_2]-K(H_2O)_2Co(CN)_6\}_n$ (**2**) ($L^{2-} = N,N'$ -bis-5-chloro-salicylidene)-1,2-diaminoethane). Crystal structures and thermostabilities of the compounds are investigated in detail. Magnetic characterizations indicate that the cyano-based linkers in **1** and **2** transmit antiferromagnetic interaction between the Mn(III) ions, and the correlations of structure and magnetism are also illustrated.

2. Experimental

2.1. Physical measurements

Elemental analyses (C, H, N) were performed on a Perkin-Elmer III elemental analyzer (USA). Infrared (IR) spectra were recorded with a Tensor 27 spectrometer (Bruker Optics, Ettlingen, Germany) in the range of $4000\text{--}400\text{ cm}^{-1}$ using powdered samples on a KBr pellets. Powder X-ray diffraction (PXRD) patterns were recorded on a Bruker D8 Advance diffractometer (Germany). Thermogravimetric measurements were performed with a Netzsch STA449C apparatus (Germany) under air atmosphere from 20 to $1000\text{ }^\circ\text{C}$. Magnetic measurements were obtained on poly-crystalline samples (10.21 mg for **1**, 14.69 mg for **2**) using a Quantum Design MPMS-XL7 SQUID magnetometer at temperatures between 1.8 and 300 K for direct current (dc) applied fields with an applied field

of 1 kOe (restrained in eicosane to prevent torquing at high fields). The experimental susceptibilities were corrected for the diamagnetism of the constituent atoms (Pascal's tables).

2.2. Synthesis

2.2.1. Starting materials

All of the reagents were purchased and used without further purification except for corresponding Schiff base ligand. The tetradentate Schiff base ligand H_2L was synthesized by mixing the 5-chloro-salicylidene and corresponding diamine (Scheme 2).

2.3. Synthesis of the Schiff base ligand H_2L

A solution of 5-chloro-salicylaldehyde (313.14 mg, 2 mmol) in hot absolute ethanol (40 ml) was added dropwise to a solution of ethylenediamine (60.00 mg, 1 mmol) in ethanol solution (10 ml). The mixture solution was stirred at $80\text{ }^\circ\text{C}$. Afterwards the mixture was cooled to room temperature, then filtered, washed with cold C_2H_5OH and recrystallized with hot C_2H_5OH . H_2L : Yellow powder, yield 87%, mp: $179.5\text{--}181.2\text{ }^\circ\text{C}$.

2.4. Synthesis of $[Mn(L)(H_2O)]ClO_4$

The manganese(III) precursor $[Mn(L)(H_2O)]ClO_4$ was obtained by mixing $Mn(OAc)_2$, H_2L and $NaClO_4$ in $CH_3OH\text{--}H_2O$ mixture with a molar ratio of 1:1:1.5, according to the method reported previously [38].

2.5. Synthesis of $[Mn(L)(\mu_{1,3}\text{-N}(\text{CN})_2)]_n$ (**1**)

A methanol solution (15 ml) containing $\text{Na}(\text{CN})_2$ (89 mg, 1.0 mmol) and H_2L (168.5 mg, 0.5 mmol) was added to a methanol solution (10 ml) of $\text{Mn}(\text{ClO}_4)_2 \cdot 6\text{H}_2\text{O}$ (181 mg, 0.5 mmol) with stirring for about 12 h at room temperature. Dark brown cubic crystals were obtained. Yield: 38% based on $\text{Mn}(\text{III})$. *Anal. Calc.* for $\text{C}_{18}\text{H}_{12}\text{Cl}_2\text{MnN}_5\text{O}_2$ ($M_r = 456.17$): C, 47.39; H, 2.65; N, 15.35. Found: C, 47.25; H, 2.59; N, 15.31%. IR (KBr) ν_s : 2887 (m), 2286 (s), 2156 (s), 1615 (vs), 1558 (m), 1475 (vs), 1448 (s), 1385 (vs), 1359 (s), 1249 (s), 809 (s), 689 (s), 632 (m).

2.6. Synthesis of $\{[Mn_2(L)_2(\text{H}_2\text{O})_2]K(\text{H}_2\text{O})_2\text{Co}(\text{CN})_6\}_n$ (**2**)

A solution of $\text{K}_3\text{Co}(\text{CN})_6$ (332.32 mg, 1.0 mmol) and triethylamine (50.5 mg, 0.5 mmol) in 20 ml of mixing solvent (methanol/water 4:1) was added dropwise to a methanol solution (10 ml) of $[Mn(L)(\text{H}_2\text{O})]\text{ClO}_4$ (255 mg, 0.5 mmol) with stirring for about 12 h at room temperature. The resulting solution was filtered, and the filtrate was kept a week in 50 ml beaker. The brown bulk crystals were obtained, washed with water and dried in air. Yield: 38% based on $\text{Mn}(\text{III})$. *Anal. Calc.* for $\text{C}_{38}\text{H}_{32}\text{Cl}_4\text{CoK}_2\text{Mn}_2\text{N}_{10}\text{O}_8$ ($M_r = 1106.45$): C, 41.25; H, 2.91; N, 12.66. Found: C, 41.18; H, 2.89; N, 12.59%. IR (KBr) ν_s : 3300 (w), 2869 (m), 2279 (s), 2125 (s), 1612 (vs), 1532 (m), 1436 (vs), 1448 (s), 1382 (vs), 1258 (s), 819 (s), 693 (s), 665 (m).

2.7. X-ray data collection and crystallography

Diffraction data for **1** and **2** were collected on a Bruker Smart Apex II CCD diffractometer equipped with graphite monochromated Mo $K\alpha$ radiation ($\lambda = 0.71073 \text{ \AA}$) using ω and ϕ scan mode at 296(2) K. Absorption correction were applied using the SADABS program. Their structures were solved by direct methods and refined with full-matrix least-squares refinements based on F^2 using SHELXS-97 and SHELXL-97 [39,40]. All non-hydrogen atoms were refined with anisotropic displacement parameters. Crystal data and structure refinement details for **1** and **2** are summarized in Table 1, selected bond lengths and angles are shown in Table S1.

Table 1
Crystal data and structure refinement summary for compounds **1** and **2**.

Compound	1	2
Empirical formula	$\text{C}_{18}\text{H}_{12}\text{Cl}_2\text{MnN}_5\text{O}_2$	$\text{C}_{38}\text{H}_{32}\text{Cl}_4\text{CoK}_2\text{Mn}_2\text{N}_{10}\text{O}_8$
Formula weight	456.17	1106.45
Crystal system	orthorhombic	monoclinic
Space group	$P2_12_12_1$	$P2_1/c$
a (Å)	10.7881 (18)	10.675 (2)
b (Å)	11.5713 (19)	13.996 (3)
c (Å)	16.461 (3)	14.975 (3)
α (°)	90	90
β (°)	90	94.029 (4)
γ (°)	90	90
V (Å ³)	2054.9 (6)	2231.9 (8)
Crystal size (mm)	$0.1 \times 0.1 \times 0.1$	$0.12 \times 0.11 \times 0.09$
Z	4	2
D_{calc} (Mg m ⁻³)	1.474	1.646
$F(000)$	920	1116
R_{int}	0.0581	0.0958
Data/restraints/parameters	3881/0/253	4437/6/298
Goodness-of-fit (GOF) on F^2	1.007	1.095
Final R indices [$I > 2\sigma(I)$]	$R_1 = 0.0473$, $wR_2 = 0.1104$	$R_1 = 0.1038$, $wR_2 = 0.2177$
R indices (all data)	$R_1 = 0.0733$, $wR_2 = 0.1365$	$R_1 = 0.1563$, $wR_2 = 0.2533$

3. Results and discussion

3.1. Synthesis and general characterization

It is a popular strategy to use the cyanide groups as bridging ligands for synthesizing the molecule-based magnets due to the high electric charge density on both donor atoms. In the context, we choose two kinds of cyanide groups including $\text{N}(\text{CN})_2^-$ and $\text{Co}(\text{CN})_6^{3-}$ as well as corresponding tetradentate Schiff base ligand (H_2L) for the explore of the magnetic coupling rule. Compounds **1** and **2** were synthesized by using the method of slow evaporation of the resulting methanol or ethanol solution. In compound **1**, the $\text{N}(\text{CN})_2^-$ group adopts $\mu_{1,3}$ bridging modes. Additionally, $\text{Mn}(\text{II})$ ions were oxidized to $\text{Mn}(\text{III})$ ions in the synthetic processes of **1** and **2**.

3.2. FTIR spectra

For compounds **1** and **2**, the IR spectra in the range 2242–2286 cm^{-1} exhibits strong and sharp peaks assigned to the asymmetric and symmetric stretching vibrations of the cyanide groups. The characteristic absorption bands in the range 1612–1628 cm^{-1} confirm the presence of $\text{C}=\text{N}$ bands in the Schiff-base, and an intense and broad peak at 2900–3100 cm^{-1} corresponds to the stretching vibrations of the $=\text{C}-\text{H}$ band in compounds **1** and **2**. Moreover, a broad peak at 3300 cm^{-1} has been observed, which represent the O–H stretching vibration of water molecule in compound **2**.

3.3. Crystal structure of compound **1**

The structure of compound **1** crystallizes in orthorhombic space group $P2_12_12_1$, which consists of several 1D chains with the $\mu_{1,3}$ - $\text{N}(\text{CN})_2^-$ bridging. There is only one crystallographically independent $\text{Mn}(\text{III})$ ion coordinated by the N_2O_2 donor atoms from one H_2L ligand in the equatorial plane and two $\text{N}(\text{CN})_2^-$ anions in the axial positions, producing a distorted octahedral geometry, as shown in Fig. 1. Normally, nearly coplanar O(1), O(2), N(1) and N(2) atoms from H_2L connect to the $\text{Mn}(\text{III})$ ion in the equatorial plane exhibiting nearly identical $\text{Mn}-\text{O}$ (1.874 Å) and $\text{Mn}-\text{N}$ (1.981 Å) bond lengths. The axial bond length between $\text{Mn}(\text{III})$ ion and N atoms from $\mu_{1,3}$ - $\text{N}(\text{CN})_2^-$ groups is 2.386 Å. This case probably attributes to the Jahn–Teller effect at the high-spin d^4 metal center, which is commonly observed in octahedral $\text{Mn}(\text{III})$ -containing compounds [41]. As shown in Fig. 2(a), $\text{N}(\text{CN})_2^-$ ligand adopts $\mu_{1,3}$ -bridging mode to connect to adjacent monomeric $[\text{Mn}(\text{L})]^+$ units, generating an extended 1D helical chain along the crystallographic b direction (Fig. 2(b)). The nearest distance between intrachain $\text{Mn}(\text{III})$ centers bridged by $\text{trans-}\mu_{1,3}$ -

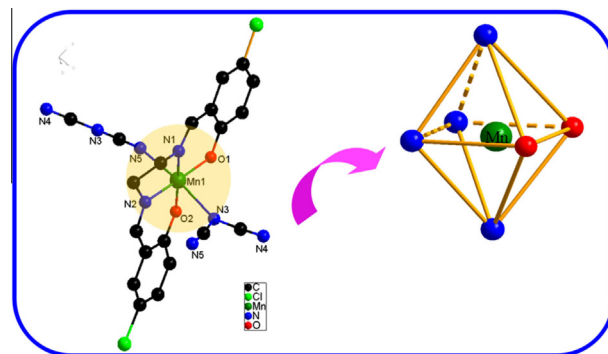


Fig. 1. Crystal structure and coordination polyhedron geometry of $\text{Mn}(\text{III})$ in **1**.

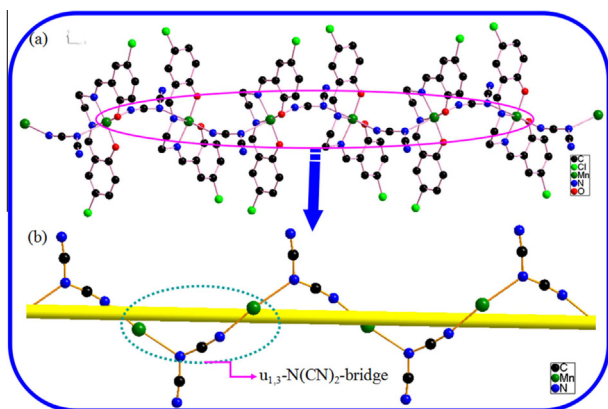


Fig. 2. (a) One-dimensional alternating chain structure of compound **1** and (b) helical chain structure along the crystallographic *b* direction.

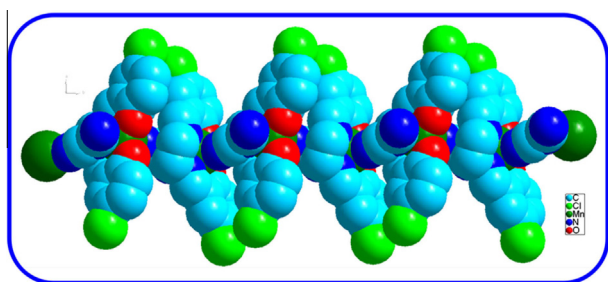


Fig. 3. RASMOL drawing of 1D helical chain by the bridging- $\text{N}(\text{CN})_2^-$ along the *c*-axis for compound **1**.

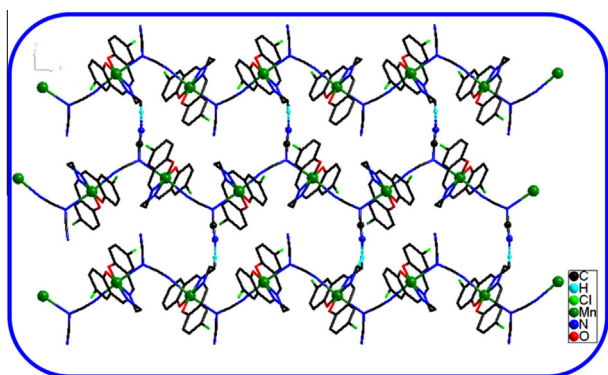


Fig. 4. Crystal packing for compound **1**.

$\text{N}(\text{CN})_2$ is about 5.5943(15) Å. The space-filling view of 1D helical chain is shown in Fig. 3. Subsequently, the large quantities of intermolecular hydrogen bonds formed by the L^{2-} ligands with free cyanido N atoms eventually link the 1D helical chain into a two-dimensional supramolecular network, as shown in Fig. 4.

3.4. Crystal structure of compound **2**

X-ray crystallography shows that compound **2** crystallizes in monoclinic space group $P2_1/c$. The asymmetric unit contains half a trinuclear ($\text{Mn}-\text{CN}-\text{Co}-\text{NC}-\text{Mn}$) unit as well as a K^+ cation and three water molecules. All Mn(III) ion centers adopt the identical distorted octahedral configuration due to the characteristic Jahn–Teller effect either, of which the equatorial plane is fixed by two amine N atoms [$\text{Mn}(1)-\text{N} = 1.989(7)$ and $1.982(8)$ Å] and

two phenolato O atoms in the Schiff base ligands [$\text{Mn}(1)-\text{O} = 1.873(6)$ and $1.882(2)$ Å] (Fig. 5). One axial position is taken up through the N atom from $\text{trans}-\text{CN}^-$ group with a long $\text{Mn}(1)-\text{N}(3)$ distance of 2.323(8) Å and a rarely case of which the $\text{Mn}(1)-\text{N}(3)-\text{C}(3)$ angle is curved to be $143.3(8)^\circ$. Another axial site is coordinated by O atom from water molecule with $\text{Mn}(1)-\text{O}(3)$ distance of 2.263(6) Å. Whereafter, a pair of $[\text{Mn}(\text{L})(\text{H}_2\text{O})]$ fragments are linked by two CN^- groups from one $\text{Co}(\text{CN})_6^{3-}$ anion assembling unique trinuclear unit of $\text{Mn}-\text{NC}-\text{Co}-\text{CN}-\text{Mn}$ [$\text{Co}(1)-\text{C}(2) = 1.914(11)$ Å, $\text{Co}(1)-\text{C}(3) = 1.888(8)$ Å, $\text{Co}(1)-\text{C}(3)-\text{N}(3) = 177.7(8)^\circ$ and $\text{N}(2)-\text{C}(2)-\text{Co}(1) = 176.8(9)^\circ$]. K^+ ion is tetra-coordinated by two N atoms from $\text{trans}-\text{CN}^-$ groups and two O atoms from water molecules [$\text{K}(1)-\text{N}(2) = 2.754(10)$ Å, $\text{K}(1)-\text{O}(5) = 2.779(12)$ Å], which further link to the adjacent trinuclear units, forming the 1D alternating chain [$\text{C}(2)-\text{N}(2)-\text{K}(1) = 135.4(8)^\circ$], as shown in Fig 6(a). Consequently, Mn(III) and K(I) centers are bridged through $\text{Co}(\text{CN})_6^{3-}$ ligands, respectively, building an interesting one-dimensional structure with ladder-like chains. The topological analysis method was used to describe and understand the structural characteristics of compound **2** intuitively (Fig 6(b)). The hydrogen bonds between water molecules and Schiff base ligands [$\text{O}(3)-\text{H}(2\text{W}) \cdots \text{O}(2) = 2.855(9)$ Å] (Table S2) combine the 1D chains to form the 2D layer and act as a crucial role for stabilizing the integrally structural framework (Fig. 7).

3.5. Thermogravimetric analysis and PXRD measurement

In order to study the thermal stabilities of compounds **1** and **2**, thermogravimetric analysis (TGA) experiment has been carried out, the samples were heated up to 1000 °C at a heating rate of 10 °C/min under a flow of nitrogen atmosphere. TG data of **1** and **2** are plotted in Fig. 8. TGA curves indicate that two compounds could be stable up to 410 °C for **1** and 195 °C for **2**. Then, only one continuous process of weight loss (80.12%) occurs in the range 410–530 °C for **1**, which is corresponding to the collapse of the main framework. Unlike **1**, compound **2** undergoes two stages of weight loss. The first course from 195 to 215 °C was described as the loss of coordination water molecules, and the second weight loss stage from 420 to 590 °C was attributed to the collapse of the main framework. The final residues are detected with the weight of 20.05% for **1** and 21.89% for **2**. It would be difficult to deduce the ultimate compositions according to the remnant mass of compounds **1** and **2**.

To confirm the phase purity of the obtained compounds **1** and **2**, the original samples were measured by PXRD at room temperature. As shown in Fig. S1, the patterns that were simulated from the single-crystal X-ray data of the compounds are in agreement with those that were observed.

3.6. Magnetic properties of **1**

The temperature dependence of the magnetic susceptibility of **1** was measured from 1.8 to 300 K in an applied magnetic field of 1 kOe (Fig. 9). In the form of $1/\chi_M$ and $\chi_M T$ versus T plots, the $\chi_M T$ value is $2.559 \text{ cm}^3 \text{ K mol}^{-1}$ at room temperature, slightly below the expected $3.0 \text{ cm}^3 \text{ K mol}^{-1}$ for an isolated high-spin Mn(III) ion ($S = 2$, $g = 2.0$). Upon lowering the temperature, the $\chi_M T$ product smoothly decreases down to 50 K and abruptly drop to the minimum value of $1.25 \text{ cm}^3 \text{ K mol}^{-1}$ for **1** at 1.8 K, which reveal definitely intrachain antiferromagnetic (AF) coupling between Mn(III) ions. The inverse magnetic susceptibility obeys the Curie–Weiss law above 10 K with the Curie constant $C = 2.614 \text{ cm}^3 \text{ K mol}^{-1}$ and Weiss constant $\theta = -4.122 \text{ K}$. The negative Weiss constants suggest that the dominant antiferromagnetic

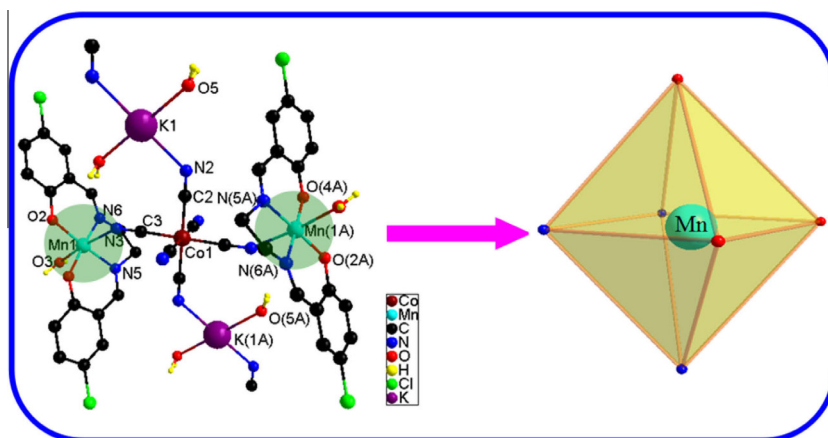


Fig. 5. Crystal structure and coordination polyhedron geometry of Mn(III) in **2**.

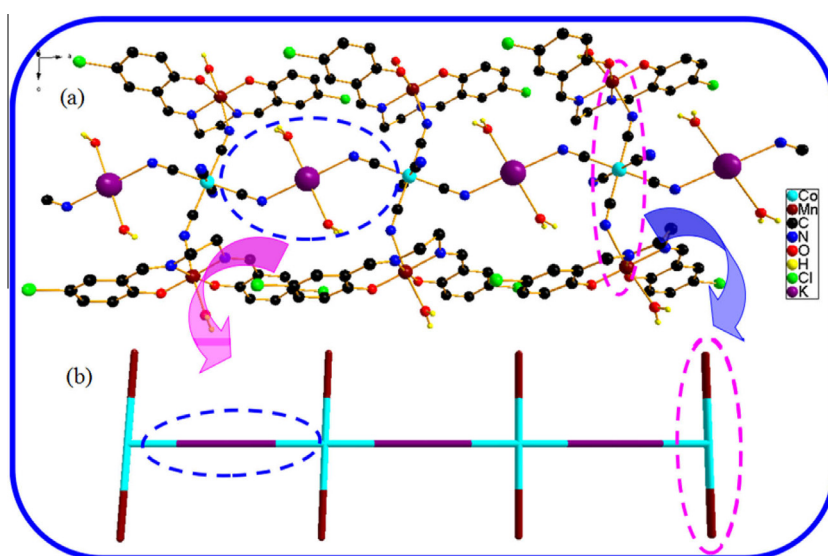


Fig. 6. (a) One-dimensional alternating chain structure of compound **2** and (b) simplified 1D structure of **2**.

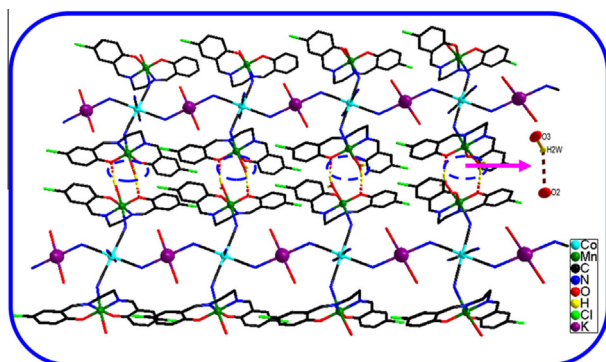


Fig. 7. 2D square networks of compound **2** was formed by the intermolecular hydrogen bonding.

coupling between adjacent Mn(III) ions exist in compound **1** with $\mu_{1,3}$ -N(CN)₂ bridges.

To probe the magnetic coupling constants J within the 1D chain, the susceptibility data of compound **1** are fitted from 300 to 10 K, and the fit of the data in terms of the uniform chain model [42,43] that includes the zero-field-splitting (D) effect for each Mn(III) ion

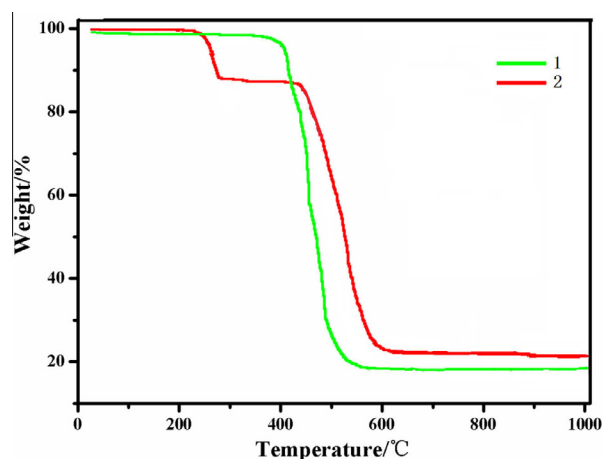


Fig. 8. TG curves of compounds **1** and **2**.

with $\hat{H} = -J\sum_i S_i \cdot S_{i+1} + \sum D_i S_i^2$. Based on the considerations above, the best least-squares fits of the experimental data are obtained as $J = -1.16 \text{ cm}^{-1}$, $g = 1.99$, $D = -2.26 \text{ cm}^{-1}$, $R = 5.62 \times 10^{-4}$ ($R = \sum [(\chi_{MT})_{\text{obsd}} - (\chi_{MT})_{\text{calcd}}]^2 / \sum [(\chi_{MT})_{\text{obsd}}]^2$) for **1**. The D value

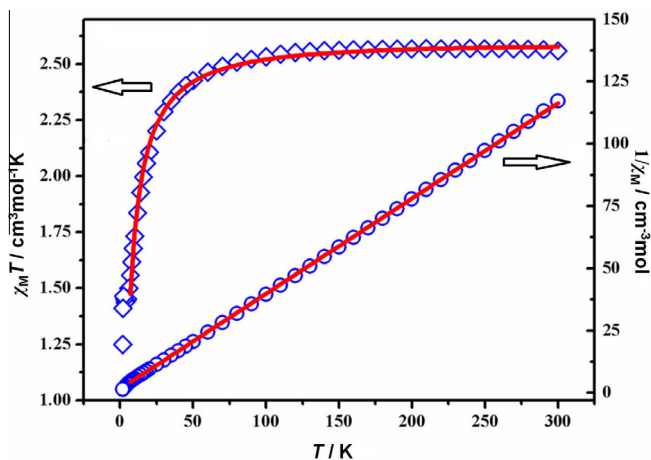


Fig. 9. $\chi_M T$ and $1/\chi_M$ vs. T plots for compound **1**. The red lines represent a best-fit. (For interpretation of the references to color in this figure legend, the reader is referred to the web version of this article.)

is consistent with the typical value for Mn(III) salen analogs and the presence of Jahn–Teller distortion in these compounds [20,44]. The negative J value further indicates the existence of intrachain antiferromagnetic exchange between the Mn(III) spins.

3.7. Magnetic properties of **2**

The magnetic property of compound **2** is reflected in Fig. 10. Due to the diamagnetic nature of the $[\text{Co(III)}(\text{CN})_6]^{3-}$ anions, compound **2** is proved to be a magnetically dilute system. The $\chi_M T$ value per Mn(III)₂Co(III) unit at room temperature is $5.942 \text{ cm}^3 \text{ K mol}^{-1}$, which is slightly less than the value of $6.0 \text{ cm}^3 \text{ K mol}^{-1}$ expected for two isolated manganese(III) ions ($S = 2$) with diamagnetic Co(III) ($S = 0$). With the decreasing of temperature, the $\chi_M T$ value remains almost constant up to 50 K, then $\chi_M T$ value sharply drop and realize a minimum of $3.152 \text{ cm}^3 \text{ K mol}^{-1}$ at 1.8 K. The magnetic susceptibility conforms closely to the Curie–Weiss law in the range of 2–300 K with a negative Weiss constant of $\theta = -1.546 \text{ K}$ and Curie constant of $C = 5.994 \text{ cm}^3 \text{ K mol}^{-1}$, suggesting the very weak antiferromagnetic coupling between Mn(III) ions.

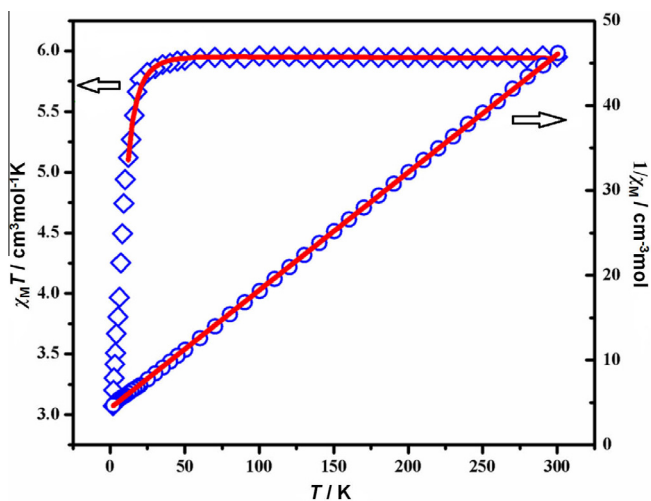


Fig. 10. $\chi_M T$ and $1/\chi_M$ vs. T plots for compound **2**. The red lines represent a best-fit. (For interpretation of the references to color in this figure legend, the reader is referred to the web version of this article.)

Like **1**, the experimental data can be modeled by using the Heisenberg model that includes the zero-field-splitting (D) effect for each Mn(III) ion. The best fit of the magnetic data is produced with the following set of parameters: $g = 2.11$, $J = -1.05 \text{ cm}^{-1}$, $D = -1.68 \text{ cm}^{-1}$ and $R = 1.52 \times 10^{-4}$ ($R = \sum[(\chi_M T)_{\text{obsd}} - (\chi_M T)_{\text{calcd}}]^2 / \sum[(\chi_M T)_{\text{obsd}}]^2$). The obtained negative J value further confirms the existence of the antiferromagnetic coupling.

3.8. Magneto-structural correlation

In summary, the characteristic of the magnetic coupling between high-spin Mn(III) ions (d^4 , t_{2g}^3 , e_g^1) through the cyanide-bridging in this work is similar to those of cyanide-bridged Mn(III) systems reported previously [37,45]. According to the GK rule [46,47], ferromagnetic and antiferromagnetic contributions coexist in the magnetic system, and the antiferromagnetic contributions that derive from the overlap of magnetic orbitals of t_{2g} symmetry between Mn(III)–Co(III) and Mn(III) ions are dominant in these systems. Hence, the antiferromagnetic interactions between Mn(III) ions transmitted by cyanide-bridging are predicted for compounds **1** and **2**. In addition, the bending of the Mn–N–C angle behaves as an important factor to affect the magnetic behaviors in the system because it diminishes the overlap of t_{2g} -type magnetic orbitals on the adjacent Mn(III) ions and therefore weakens the antiferromagnetic contributions. According to the study previously, it is indicated that the Mn–N–C angle close to 150° tends to perform ferromagnetic coupling [48]. Obviously, the Mn–N–C angles of compounds **1** and **2** in this work deviate from the angle of 150° [$(\text{Mn–N–C})_{\text{av}} = 160^\circ$ for **1**, $(\text{Mn–N–C})_{\text{av}} = 140^\circ$ for **2**], which lead to antiferromagnetic coupling between the Mn(III) ions.

4. Conclusions

In present work, based on $[\text{Mn}(\text{SB})]^{+}$ building blocks and two different bridging ligands of $\text{N}(\text{CN})_2^-$ and $\text{Co}(\text{CN})_6^{3-}$ groups, we have successfully synthesized and characterized two compounds with 1D helical structure and novel 1D ladder-like structure, respectively. Structural analyses reveals that the manganese center adopts hexa-coordinated geometry with typical Jahn–Teller distortion in two compounds which display remarkable thermostabilities with the decomposition temperatures up to 410°C and 195°C , respectively. Magnetic investigation indicates that the cyanide-bridges transmit antiferromagnetic interaction between Mn(III) ions in **1** and **2**. The title compounds may be used as building blocks in designing and developing advanced magnetic materials.

Acknowledgement

We gratefully acknowledge the financial support from the National Natural Science Foundation of China (Grant Nos. 21373162, 21463020 and 21173168), and the Nature Science Foundation of Shaanxi Province (Grant Nos. 11JS110, FF10091 and SJ08B09).

Appendix A. Supplementary material

Selected bond lengths (\AA), bond angles ($^\circ$) for **1** and **2** are in the supporting information. CCDC 987929 and 987930 contains the supplementary crystallographic data for compounds **1** and **2**, respectively. These data can be obtained free of charge from The Cambridge Crystallographic Data Centre via www.ccdc.cam.ac.uk/data_request/cif. Supplementary data associated with this article can be found, in the online version, at <http://dx.doi.org/10.1016/j.ica.2014.09.009>.

References

- [1] A. Das, K. Gieb, Y. Krupskaya, S. Demeshko, S. Dechert, R. Klingeler, V. Kataev, B. Buchner, P. Müller, F. Meyer, *J. Am. Chem. Soc.* 133 (2011) 3433.
- [2] I.J. Hewitt, J. Tang, N.T. Madhu, C.E. Anson, Y. Lan, J. Luzon, M. Etienne, R. Sessoli, A.K. Powell, *Angew. Chem., Int. Ed.* 49 (2010) 6352.
- [3] S. Ferlay, T. Mallah, R. Ouahes, P. Veillet, M. Verdaguer, *Nature* 378 (1995) 701.
- [4] S.-D. Jiang, B.-W. Wang, G. Su, Z.-M. Wang, S. Gao, *Angew. Chem., Int. Ed.* 49 (2010) 7448.
- [5] O. Sato, T. Iyoda, A. Fujishima, K. Hashimoto, *Science* 272 (1996) 704.
- [6] B.-Q. Ma, S. Gao, G. Su, G.-X. Xu, *Angew. Chem., Int. Ed.* 40 (2001) 434.
- [7] J. Larionova, J. Sanchiz, S. Gohlen, L. Ouahab, O. Kahn, *Chem. Commun.* 9 (1998) 953.
- [8] M. Yuan, F. Zhao, W. Zhang, F. Pan, Z.-M. Wang, S. Gao, *Chem. Eur. J.* 13 (2007) 2937.
- [9] L. Bogani, A. Vindigni, R. Sessoli, D.J. Gatteschi, *Mater. Chem.* 18 (2008) 4750.
- [10] T.D. Harris, M.V. Bennett, R. Clerac, J.R. Long, *J. Am. Chem. Soc.* 132 (2010) 3980.
- [11] L. Sorace, C. Sangregorio, A. Figuerola, C. Benelli, D. Gatteschi, *Chem. Eur. J.* 15 (2009) 1377.
- [12] O. Kahn, *Molecular Magnetism*, VCH, Weinheim, Germany, 1993.
- [13] O. Sato, T. Kawakami, M. Kimura, S. Hishiyama, S. Kubo, Y. Einaga, *J. Am. Chem. Soc.* 126 (2004) 13176.
- [14] C.P. Berlinguette, A. Dragulescu-Andrasi, A. Sieber, J.R. Galan-Mascaros, H.U. Gudel, C. Achim, K.R. Dunbar, *J. Am. Chem. Soc.* 126 (2004) 6222.
- [15] M. Shatruk, A. Dragulescu-Andrasi, K.E. Chambers, S.A. Stoian, E.L. Bominaar, C. Achim, K.R. Dunbar, *J. Am. Chem. Soc.* 129 (2007) 6104.
- [16] S. Nayak, M. Evangelisti, A.K. Powell, J. Reedijk, *Chem. Eur. J.* 16 (2010) 12865.
- [17] A. Escuer, G. Aromí, *Eur. J. Inorg. Chem.* 23 (2006) 4721.
- [18] R.-Y. Li, Z.-M. Wang, S. Gao, *Crystallogr. Eng. Comm.* 11 (2009) 2096.
- [19] X.-Y. Wang, Z.-M. Wang, S. Gao, *Chem. Commun.* 3 (2008) 281.
- [20] B.J. Kennedy, K.S. Murray, *Inorg. Chem.* 24 (1985) 1552.
- [21] H.-L. Sun, Z.-M. Wang, S. Gao, *Inorg. Chem.* 44 (2005) 2169.
- [22] K. Bha, S. Das, S. Satapathi, P. Mitra, J. Ribas, B.K. Ghosh, *Polyhedron* 29 (2010) 2041.
- [23] S.-W. Choi, H.-Y. Kwak, J.-H. Yoon, H.-C. Kim, E.-K. Koh, C.-S. Hong, *Inorg. Chem.* 47 (2008) 10214.
- [24] T.D. Harris, C. Coulon, R. Clerac, J.R. Long, *J. Am. Chem. Soc.* 133 (2011) 123.
- [25] R. Garde, F. Villain, M. Verdaguer, *J. Am. Chem. Soc.* 124 (2002) 10531.
- [26] Ø. Hatlevik, W.E. Buschmann, J. Zhang, J.L. Manson, J.S. Miller, *Adv. Mater.* 11 (1999) 914.
- [27] H.J. Choi, J.J. Sokol, J.R. Long, *Inorg. Chem.* 43 (2004) 1606.
- [28] E.J. Schelter, A.V. Prosvirin, K.R. Dunbar, *J. Am. Chem. Soc.* 126 (2004) 15004.
- [29] D. Visinescu, A.M. Madalan, M. Andruh, C. Duhayon, J.P. Sutter, L. Ungur, W. Van den Heuvel, L.F. Chibotaru, *Chem. Eur. J.* 15 (2009) 11808.
- [30] L.M. Toma, R. Lescouëzec, F. Lloret, M. Julve, J. Vaissermann, M. Verdaguer, *Chem. Commun.* (2003) 1850.
- [31] B.-W. Sun, S. Gao, B.-Q. Ma, D.-Z. Niu, Z.-M. Wang, *J. Chem. Soc., Dalton Trans.* (2000) 4187.
- [32] C. Avendano, F. Karadas, M. Hilfiger, M. Shatruk, R. Dunbar Kim, *Inorg. Chem.* 49 (2010) 583.
- [33] M. Hirotsu, K. Nakajima, M. Kojima, Y. Yoshikawa, *Inorg. Chem.* 34 (1995) 6173.
- [34] N. Re, R. Crescenzi, C. Floriani, H. Miyasaka, N. Matsumoto, *Inorg. Chem.* 37 (1998) 2717.
- [35] Q. Shi, R. Cao, X. Li, J.-H. Luo, M.-C. Hong, Z.-N. Chen, *New J. Chem.* 26 (2002) 1397.
- [36] C.J. Milios, A. Vinslava, P.A. Wood, S. Parsons, W. Wernsdorfer, G. Christou, S.P. Perlepes, E.K. Brechin, *J. Am. Chem. Soc.* 129 (2007) 8.
- [37] M. Yuan Zhao, F.-W. Zhang, Z.-M. Wang, S. Gao, *Inorg. Chem.* 46 (2007) 11235.
- [38] P. Przychodzeń, K. Lewiński, M. Balanda, R. Pelka, M. Rams, T. Wasutyński, C. Guyard-Duhayon, B. Sieklucka, *Inorg. Chem.* 43 (2004) 2967.
- [39] G.M. Sheldrick, *SHELXS-97*, Program for Solution of Crystal Structures, University of Göttingen, Germany, 1997.
- [40] G.M. Sheldrick, *SHELXL-97*, Program for Solution of Crystal Structures, University of Göttingen, Germany, 1997.
- [41] H.-K. Hyun, H.-L. Jeong, C.-K. Hyoung, S.-H. Chang, *Inorg. Chem.* 45 (2006) 8847.
- [42] G.R. Wagner, S.A. Friendberg, *Phys. Lett.* 9 (1964) 11.
- [43] M.E. Fisher, *Am. J. Phys.* 32 (1964) 343.
- [44] H. Miyasaka, R. Clérac, T. Ishii, H.-C. Chang, S. Kitagawa, M.J. Yamashita, *Chem. Soc., Dalton Trans.* (2002) 1528.
- [45] B. Samanta, J. Chakraborty, B.R.K. Singh, M.K. Saha, S.R. Batten, P. Jensen, M.S.E. Fallah, S. Mitra, *Polyhedron* 26 (2007) 4354.
- [46] J.B. Goodenough, *Phys. Rev.* 100 (1955) 564.
- [47] J. Kan-amori, *J. Phys. Chem. Solids* 10 (1959) 87.
- [48] H. Miyasaka, H. Takahashi, T. Madanbashi, K.I. Sugiura, R. Clérac, H. Nojiri, *Inorg. Chem.* 43 (2005) 5969.